

Accepted Manuscript

Quinolone antibiotic derivatives as new selective Axl kinase inhibitors

Li Tan, Zhang Zhang, Donglin Gao, Shingpan Chan, Jinfeng Luo, Zheng-Chao Tu, Zhi-Min Zhang, Ke Ding, Xiaomei Ren, Xiaoyun Lu



PII: S0223-5234(19)30085-6

DOI: <https://doi.org/10.1016/j.ejmech.2019.01.065>

Reference: EJMECH 11072

To appear in: *European Journal of Medicinal Chemistry*

Received Date: 21 December 2018

Revised Date: 27 January 2019

Accepted Date: 27 January 2019

Please cite this article as: L. Tan, Z. Zhang, D. Gao, S. Chan, J. Luo, Z.-C. Tu, Z.-M. Zhang, K. Ding, X. Ren, X. Lu, Quinolone antibiotic derivatives as new selective Axl kinase inhibitors, *European Journal of Medicinal Chemistry* (2019), doi: <https://doi.org/10.1016/j.ejmech.2019.01.065>.

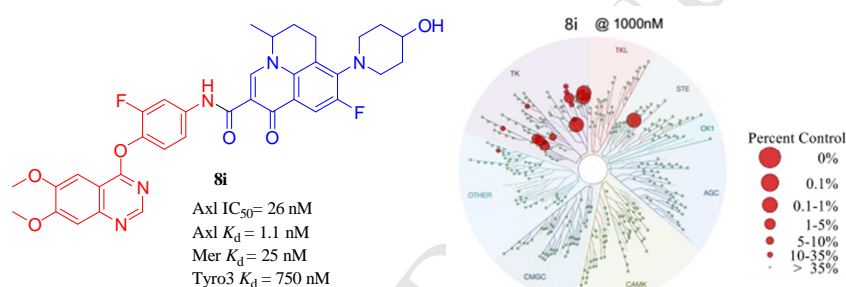
This is a PDF file of an unedited manuscript that has been accepted for publication. As a service to our customers we are providing this early version of the manuscript. The manuscript will undergo copyediting, typesetting, and review of the resulting proof before it is published in its final form. Please note that during the production process errors may be discovered which could affect the content, and all legal disclaimers that apply to the journal pertain.

Quinolone Antibiotic Derivatives as New Selective Axl Kinase Inhibitors

Li Tan^{a,#}, Zhang Zhang^{a,#}, Donglin Gao^{b,#}, Shingpan Chan^a, Jinfeng Luo^b, Zheng-Chao Tu^b, Zhi-Min Zhang^a, Ke Ding^a, * Xiaomei Ren^{a,*}, Xiaoyun Lu^{a,*}

^aInternational Cooperative Laboratory of Traditional Chinese Medicine Modernization and Innovative Drug Development, Ministry of Education (MOE) of People's Republic of China and Guangzhou City Key Laboratory of Precision Chemical Drug Development, School of Pharmacy, Jinan University, 601 Huangpu Avenue West, Guangzhou, 510632, China

^bState Key Laboratory of Respiratory Diseases, Guangzhou Institutes of Biomedicine and Health, Chinese Academy of Sciences, 190 Kaiyuan Avenue, Guangzhou 510530, China



Compound **8i** bound to Axl with a K_d value of 1.1 nM, and inhibited its kinase activity with an IC₅₀ value of 26 nM. Further, **8i** exhibited extraordinary target selectivity over 468 kinases, with a S(10) and S(35) value of 0.022 and 0.42 at 1.0 μM, and significantly inhibited the phosphorylation of Axl and dose dependently inhibited cell invasion and migration in TGF-β1 induced MDA-MD-231 breast cancer cells.

Quinolone Antibiotic Derivatives as New Selective Axl Kinase

Inhibitors

Li Tan^{a,#}, Zhang Zhang^{a,#}, Donglin Gao^{b,#}, Shingpan Chan^a, Jinfeng Luo^b, Zheng-Chao Tu^b, Zhi-Min Zhang^a, Ke Ding^{a,*}, Xiaomei Ren^{a,*}, Xiaoyun Lu^{a,*}

^a International Cooperative Laboratory of Traditional Chinese Medicine Modernization and Innovative Drug Development, Ministry of Education (MOE) of People's Republic of China and Guangzhou City Key Laboratory of Precision Chemical Drug Development, School of Pharmacy, Jinan University, 601 Huangpu Avenue West, Guangzhou, 510632, China

^b Guangzhou Institutes of Biomedicine and Health, Chinese Academy of Sciences, 190 Kaiyuan Avenue, Guangzhou 510530, China

Corresponding authors: Tel: +86-20-85221523. E-mail: ding_ke@gibh.ac.cn; ren_xiaomei@jnu.edu.cn; luxy2016@jnu.edu.cn.

Abstract

Axl is a new promising molecular target for antineoplastic therapies. A series of quinolone antibiotic derivatives were designed and synthesized as new selective Axl inhibitors. One of the most promising compound **8i** bound tightly to Axl with a K_d value of 1.1 nM, and inhibited its kinase activity with an IC_{50} value of 26 nM. The compound also significantly inhibited the phosphorylation of Axl and dose dependently inhibited cell invasion and migration in TGF- β 1 induced MDA-MD-231 breast cancer cells. In addition, **8i** demonstrated reasonable pharmacokinetic properties and exhibited extraordinary target selectivity over 468 kinases except for Flt3 (IC_{50} = 50 nM), with a S(10) and S(35) value of 0.022 and 0.42 at 1.0 μ M, respectively. Compound **8i** may serve as a new valuable lead compound for future anticancer drug discovery.

Keyword: Axl, quinolones, selective inhibitor, breast cancer

1. Introduction

Axl is a tyrosine kinase that belongs to TAM subfamily which consists of three highly conserved members (i.e., Tyro3, Axl and c-mer proto-oncogene tyrosine kinase (Mer)) [1]. Upon binding with the endogenous ligand growth arrest-specific 6 (Gas6), Axl activates various signal transduction cascades (e.g. PI3K/Akt, MEK/ERK and SOCS/STAT etc) to mediate a number of fundamental cellular processes including cell growth and survival, proliferation, differentiation,

cell adhesion and migration, invasion and angiogenesis etc [2]. Over-expression and/or over-activation of Axl is frequently detected in a variety of human tumors, and closely correlated to tumor aggressiveness and drug resistance [3-5]. Dysregulation of Axl correlates with poor prognosis in various types of human cancer. For instance, increasing levels of Axl and Gas6 are frequently found and Axl is one of most phosphorylated RTKs in over 50% of non-small cell lung cancer cells (NSCLCs) [6-7]. Recent results also indicated that up-regulation of Axl tends to be closely correlated to lymph node metastasis and poor survival of NSCLC patients and is one of the important mechanisms mediated resistance to EGFR-targeted therapies [8]. The pathological role of Axl in breast cancer has also been evidenced by its prominent role to trigger epithelial-mesenchymal transition (EMT) and mediate the clinical resistance against lapatinib and trastuzumab in Her2+ and/or ER+ breast cancer patients [9]. Most recent studies revealed that Axl is closely associated with the expression of programmed death-ligand 1 (PD-L1) and inhibition of Axl led to significant reduction of PD-L1 expression under basal conditions, suggesting its promising potential in cancer immunotherapy [10]. Collectively, Axl becomes a new attractive molecular target for anti-neoplastic drug discovery [11].

A number of well characterized small molecule kinase inhibitors, e.g. NPS-1034 (**1**) [12] and Gilteritinib (**2**) [13] were reported to exhibit potent Axl inhibition activity (Figure 1), but few of them was developed by using Axl as the primary target. Several classes of selective Axl kinase inhibitors were also developed, among which TP0903 (**3**) [14] and R428 (BGB324, **4**) [15] (Figure 1) have been advanced into different stages of clinical investigation. Particularly, inhibitor **4**, which is recognized as first selective Axl inhibitor with an IC₅₀ value of 14.0 nM, was granted as “orphan-drug” designation for treatment of acute myeloid leukemia (AML) in 2014 [16]. Most recently, drug **4** also met the first efficacy endpoint in a phase II clinical trial in NSCLC patients by combination with erlotinib [17]. However, Myers and our previous work independently demonstrated that inhibitor **4** is actually also target other kinases (e.g. RET, VEGFR2 and Flt3) as potently as Axl [18-19]. Thus, it is in urgent need to discovery a more selective Axl inhibitor to explore the biological function of Axl. We have designed and synthesized a series of 4-oxo-1,4-dihydroquinoline-3-carboxamides as novel selective Axl inhibitors (**5**, Figure 2) in which a substituted quinazoline was utilized as a potential hinge region binding moiety and a quinolone was adapted as a “dual hydrogen bond acceptor (DHBA) group [19]. Further improving the

pharmacokinetic properties of **5** led to compound **6** with potent Axl inhibitory activity and ideal pharmacokinetic property, which indicated that a hydrophilic group as large as N-methyl piperazine is tolerant in the DHBA region (Figure 2). This promising result inspired us that quinolone antibiotics with similar hydrophilic group may be utilized as favourable substitutes for the DHBA segment of **6**. Quinolone represents the pharmacophore of an important class of FDA approved antibiotics, including ciprofloxacin, enoxacin, sarafloxacin, and marbofloxacin etc [20]. Following James Black's famous saying "the most fruitful basis of the discovery of a new drug is to start with an old drug" [21], we introduced clinically used quinolone drugs into compound **6** as a "DHBA group" and successfully obtained a new class of quinolone-based selective Axl inhibitors (Figure 2).

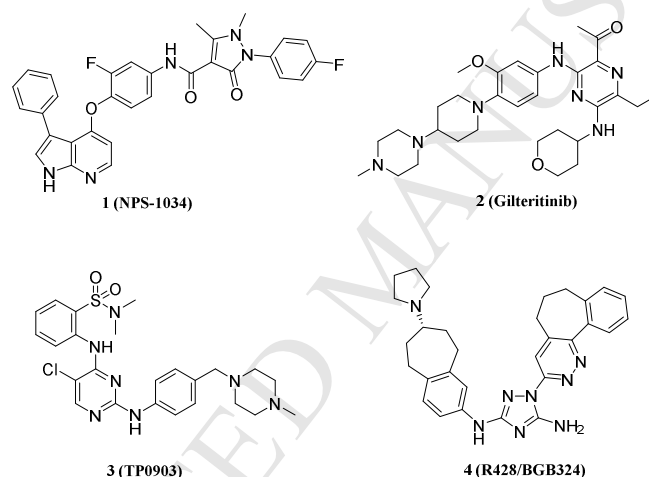


Figure 1. Chemical structures of reported Axl inhibitors.

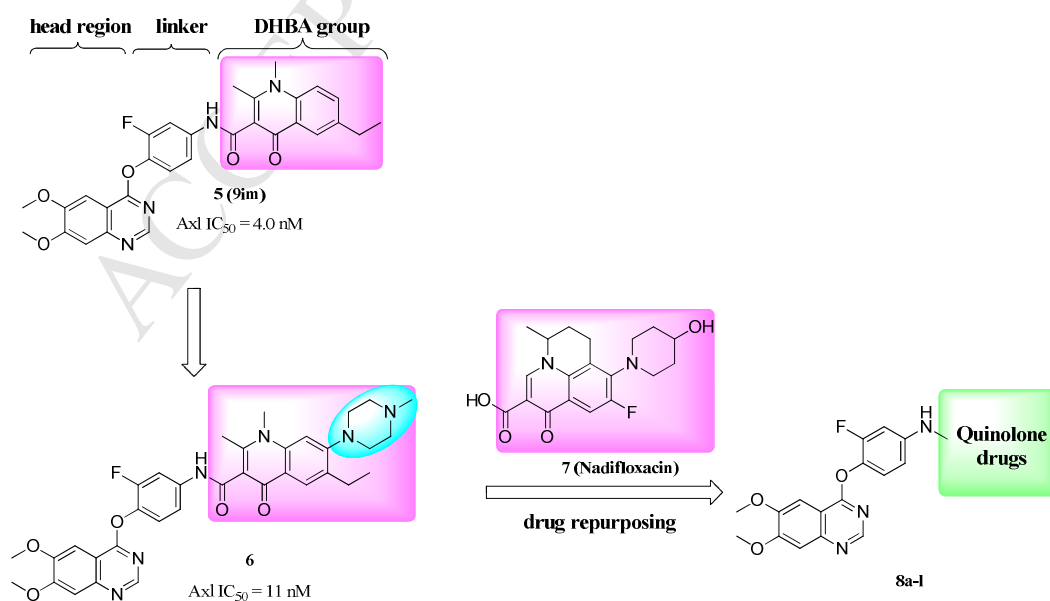
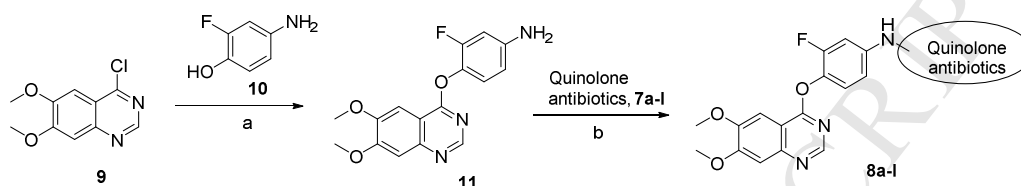


Figure 2. Design of the new potential selective Axl inhibitors

2. Chemistry

The designed compounds were readily synthesized *via* a protocol outlined in Scheme 1. Briefly, commercially available 4-chloro-6,7-dimethoxyquinazoline (**9**) was treated with 4-amino-2-fluorophenol (**10**) to yield compound **11** by a nucleophilic substitution. Intermediate **11** was then condensed with various FDA approved quinolone antibiotics (**7**) to afford the final products **8** in good yields



Scheme 1. Synthesis of compounds **8a-l**. Reagents and conditions: (a) Sodium hydride (NaH), N,N-dimethylformamide (DMF), 0 °C, 75%; (b) 2-(7-aza-1H-benzotriazol-1-yl)-1,1,3,3-tetramethyluronium hexafluorophosphate (HATU), ethyl diisopropylamine (DIPEA), DMF, room temperature (rt), overnight, 75-90%.

3. Results and Discussion

Kinase inhibitory activities of the designed compounds against Axl were evaluated via a well-established fluorescence resonance energy transfer (FRET)-based Z'-Lyte assays [22]. Inhibitor **4** was utilized as a positive control to validate the screening conditions. Under the experimental conditions, **4** exhibited strong inhibitory potency against Axl with an IC₅₀ value of 8.8 nM, which is similar to the reported data (Table 1) [15].

Table 1. *In Vitro* Axl Kinase Inhibitory Activities of Inhibitors **8a-l**.^a

Cpds	Quinolone antibiotics	Axl (IC ₅₀ , μM)	Cpds	Quinolone antibiotics	Axl (IC ₅₀ , μM)
8a		0.020	8h		0.054
8b		0.230	8i		0.026

8c		0.068	8j		0.059
8d		0.042	8k		1.246
8e		0.787	8l		0.024
8f		0.149	7	-	>10
8g		0.035	11	-	>10
4	-	0.0088	6	-	0.011

^a Axl kinase inhibition was determined by using an FRET-based Z'-Lyte assay according to the manufactory's instructions (Invitrogen, Carsbad, USA). The compounds were incubated with the kinase reaction mixture for 1.0-1.5 h before measurement. Reported data are means from 3 independent experiments in which the variation is less than 20%.

All of the designed compounds exhibited potent kinase activity against Axl with IC₅₀ values ranged from 0.020 μM to 1.25 μM (Table 1). It was also shown that the quinolone antibiotics with mono-substituted piperazine group or free amino or hydroxyl group, such as ciprofloxacin (**8a**), enoxacin (**8d**), sarafloxacin (**8g**), tosufloxacin (**8h**), nadifloxacin (**8i**) and the intermediate of prulifloxacin (**8l**), displayed favourable Axl inhibitory activities (IC₅₀ = 0.020-0.054 μM). While the derivatives of quinolone antibiotics with N-substituted (**8b**, **8f** and **8k**) or steric hindrance piperazine (**8e**) displayed less potency. We also determined the Axl inhibitory activity of compound **11** and quinolone antibiotic **7i**. The results showed that both **11** and **7i** have no inhibitory activity against Axl kinase, thus confirmed the contribution of quinolone block on Axl inhibitory activity of designed compounds. Taken into consideration both the kinase inhibitory potency and structural novelty, we chose **8i** to do further evaluation.

The binding affinity of compound **8i** with Axl protein was further determined using an active-site-dependent competition binding assay (conducted by DiscoverX Corporation, San Diego, USA) [23]. It was shown that compound **8i** tightly bound to Axl with a binding constant (K_d) value of 1.1 nM. We also profiled the target selectivity of **8i** against a panel of 468 kinases

(including 403 non-mutated kinases) using the DiscoverRx screening platform at a concentration of 1.0 μM , which is approximately 909 times higher than its K_d value against Axl. The results revealed that **8i** displayed excellent target selectivity with S(1), S(10) and S(35) scores of 0.01, 0.022 and 0.042, respectively (Table S1). The major “off target” hits included colony stimulating factor-1 receptor (CSF1R), discoidal domain receptor 1 (DDR1), DDR2, FMS-like tyrosine kinase 3 (Flt3), v-kit Hardy-Zuckerman 4 feline sarcoma viral oncogene homolog (Kit), serine/threonine kinase 10 (LOK) and nerve growth factor receptor A (TrkA) etc (Supporting Information). The binding affinities (K_d) or kinase inhibitory activities (IC_{50}) of compound **8i** against these “off targets” were further determined by using DiscoverRx’s platform or our in-house kinase assays (Table 2). It was shown that compound **8i** exhibited an approximately 25~1000-fold less potency against the majority of the “off target” kinases, with the exception of Flt3 and LOK, which displayed an IC_{50} value of 50 nM and a K_d value of 8 nM, respectively. The binding affinities of **8i** with the other TAM tyrosine kinase members (Tyro3 and Mer) were also determined. It was shown that **8i** exhibited a 25 fold less potency against Mer with a K_d value of 25 nM, while it was much less potent to Tyro3 with a K_d value of 750 nM. These results collectively supported that compound **8i** achieved an obviously better target selectivity than the positive control **4** at the same concentration (Figure 3).

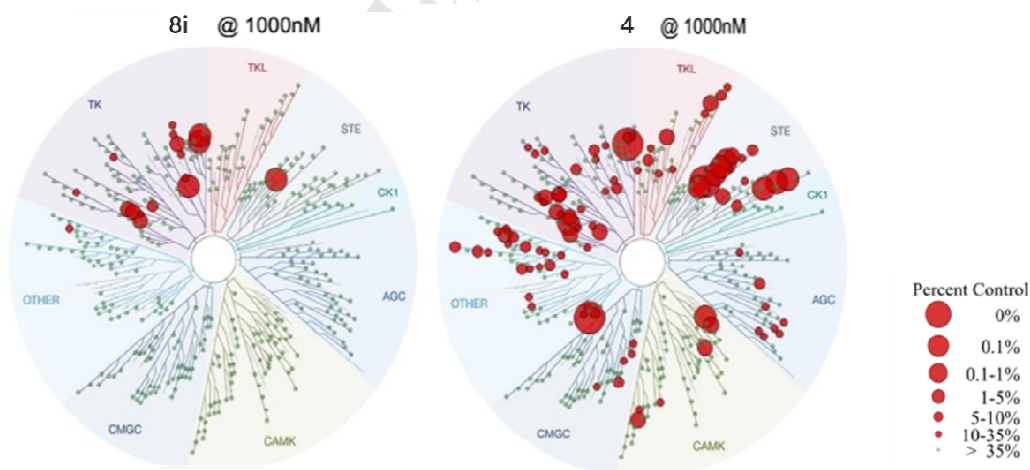


Figure 3. KINOMEScan kinase selectivity profiles of **8i** and **4** (R428).

Table 2. Binding affinities or kinase inhibition of compound **8i** against a panel of “off target” kinases.

Kinase	K_d or IC_{50} (μM)	Kinase	K_d or IC_{50} (μM)
--------	---------------------------------------------	--------	---------------------------------------------

Axl	0.001 ^a /0.026 ^b	KIT	>10 ^b
ABL	>10 ^b	LOK	0.008 ^a
AKT1/2/3	>10 ^b	MER	0.025 ^a
CSF1R	>10 ^b	PDGFRA	>10 ^b
DDR1	>10 ^b	PDGFRB	0.793 ^b
DDR2	>10 ^b	TRKA	0.125 ^b
EGFR	>10 ^b	TYRO3	0.750 ^a
Flt3	0.050 ^b	ZAK	>10 ^b

^a The binding affinities (K_d) were determined by using DiscoverX's platform. ^b The kinase inhibitory activities (IC_{50}) were evaluated by using "in-house" kinase assays. Reported data are means from 3 independent experiments in which the variation is less than 20%.

The Axl inhibitory effect of compound **8i** on the activation of Axl and downstream Akt signal was also validated by determining the phosphorylation level of Axl and Akt in MDA-MB-231 breast cancer cells which expressing a high level of Axl (Figure 4). The results revealed that **8i** dose-dependently inhibited the phosphorylation of Axl (pAxl (Tyr702)) and the downstream Akt (pAkt(Thr308)) at a low concentration, while the total amount of corresponding proteins remained unchanged as determined by western blot analysis in MDA-MB-231 cancer cells.

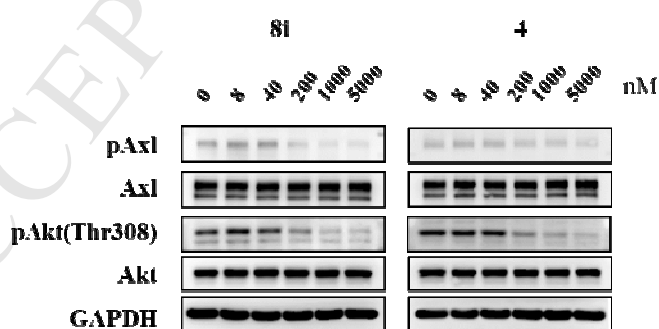


Figure 4. Compound **8i** and **4** inhibits activation of Axl and its downstream signaling pathway in MDA-MB-231 cells. The cells were treated with or without compound **8i** or **4** for 4h at the indicated concentrations, respectively.

It is well documented that Axl is closely involved in the tumor cell EMT transition process. In breast cancer, Axl was identified as an EMT induced effector to participate in a positive feedback

loop that sustains the malignant mesenchymal phenotype of breast tumor cells [24]. As transforming growth factor beta receptor (TGF- β 1) is a widely recognized EMT inducer [25], therefore, the potential antitumor activity of **8i** was further validated by determining the levels of EMT associated proteins in MDA-MB-231 cells (Figure 5). As expected, TGF- β 1 treatment significantly induced EMT process as determined by the expression level of EMT markers (a decrease of epithelial cell biomarker E-cadherin and increase of mesenchymal cell marker N-cadherin). The results also revealed that treatment of **8i** dose dependently increases the expression of epithelial marker E-cadherin and decreases the expression of mesenchymal marker N-cadherin in MDA-MB-231 cells as determined by western blot analysis, which suggested **8i** can reverse TGF- β 1 induced expression of the EMT markers in a dose dependent manner.

It has been demonstrated that EMT mediated Axl up-regulation is essential for breast cancer invasiveness and metastasis [24]. Thus, encouraged by its promising repressing ability on the TGF- β 1 induced EMT transition, we also determined the suppression activity of **8i** on TGF- β 1 induced tumor migration by a well-established transwell assay. It was shown that treatment of compound **8i** moderately inhibited the migrating process in MDA-MB-231 cells, suppressing the TGF- β 1 (10 ng/mL) induced cell migration by ~14.9%, and 69.7% at concentrations of 1.0 and 5.0 μ M, respectively, compared with the untreated control (Figures 6A, 6B). We further evaluated the inhibitory effect of **8i** on the invasiveness of MDA-MB-231 breast cancer cells by using a matrigel mediated Boyden chamber assay. It was shown that compound **8i** dose-dependently inhibited the invasiveness of MDA-MB-231 cancer cells. Treatment of **8i** at 0.04, 0.2, 1.0 or 5.0 μ M for 24 hours inhibited cancer cell invasion by ~17.4%, ~34.4%, ~73.8% and ~90.3%, respectively (compared to the TGF- β 1 (10 ng/mL) treatment; Figures 6A and 6C). These results collectively suggested the promising potential of compound **8i** to serve as a lead compound for further drug discovery.

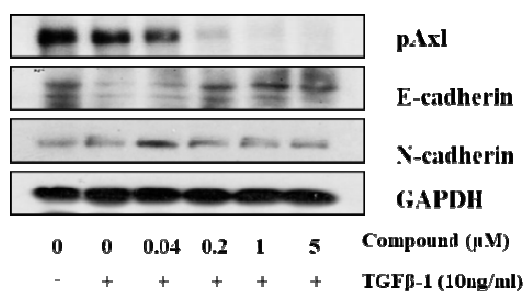


Figure 5. Compound **8i** reverses the expression of the EMT markers induced by TGF- β 1 in MDA-MB-231 cells as determined by western blot analysis.

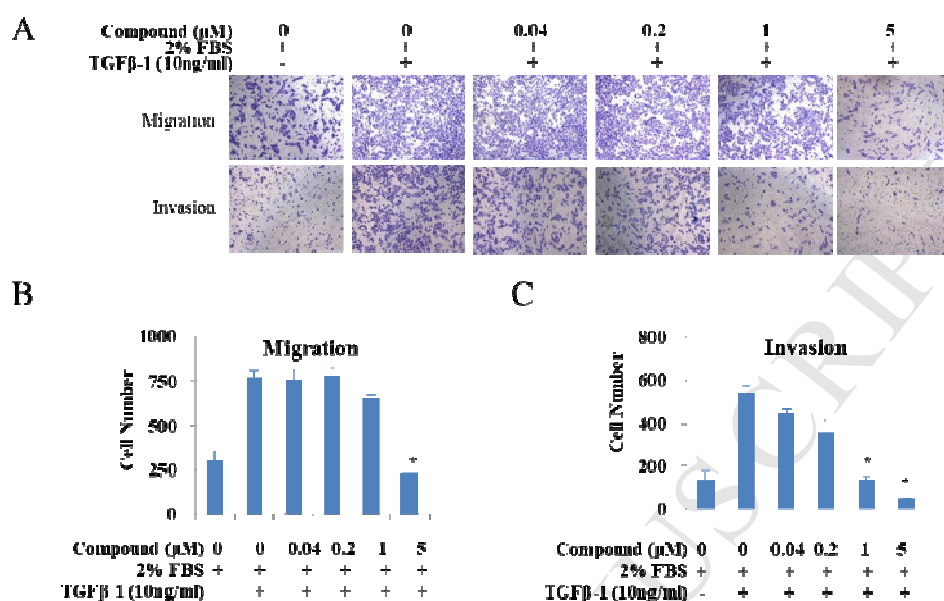


Figure 6. Compound **8i** suppresses migration and invasion of MDA-MB-231 cells. (A) Compound **8i** suppresses migration and invasion induced by TGF- β 1 (10 ng/mL) in MDA-MB-231 cells. (B, C) Quantity analysis of migration (B) and invasion (C). The results are presented as the mean \pm standard deviation, * P <0.05 (compare with TGF- β 1 treatment).

Given the promising Axl inhibitory activity *in vitro*, we further investigated preliminary *in vivo* pharmacological properties of **8i** in Sprague-Dawley (SD) rats (Table 3). Plasma levels of the compounds were monitored after a single oral dose of 25 mg/kg or an i.v. dose of 2.5 mg/kg. The results showed that, **8i** exhibited reasonable pharmacokinetic (PK) properties with an area under concentration–time curve ($AUC_{(0-\infty)}$) value of 25944.7 μ g/L*h and a $T_{1/2}$ value of 5.68 h at an oral dose of 25 mg/kg. The C_{max} (2386.9 μ g/L=3.6 μ M) occurred at 4.0 h postdose, which was 138 times higher than its IC_{50} value against Axl kinase.

Table 3. Pharmacokinetic profile of compound **8i** in SD rats

	8i	
	oral (25 mg/kg)	i.v. (2.5 mg/kg)
$AUC_{(0-\infty)}$ (μ g/L*h)	25944.7	20680.6
C_{max} (μ g/L)	2386.9	4358.2

T1/2 (h)	5.68	4.26
Tmax (h)	4.0	-
CLz (L/h/kg)	--	0.12
BA (%)	12.5%	--

Moreover, **8i** was well tolerated and there was no animal death or obvious body weight change and obvious toxicity to liver and kidney after the mice received 200 mg/kg, 400 mg/kg or 800 mg/kg administration of **8i** (Tables 4 and Figure 7). These results suggested that, **8i** may serve as a start point for further drug discovery.

Table 4. **8i** has no effects on survival and weight of ICR mice

Dose(mg/Kg)	Number		Weight(g)	
	0d	7d	0d	7d
0	6	6	23.8±0.9	27.9±1.1
50	6	6	23.5±1.2	27.7±1.5
100	6	6	23.9±1.2	27.6±1.6
200	6	6	23.3±0.9	25.8±1.2
400	6	6	23.7±1.1	26.1±1.3
600	6	6	23.9±1.2	25.6±1.5
800	6	6	24.1±1.3	25.2±1.6

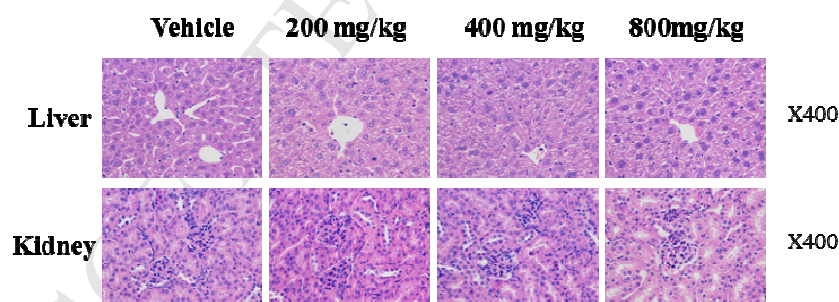


Figure 7. HE staining showed that **8i** had no obviously toxicity to liver and kidney. ICR mice were singly treated with vehicle or **8i**, then the tissues of liver and kidney were harvested after 7 days for HE staining.

4. Conclusion

In summary, a series of quinolone antibiotic derivatives were designed and synthesized as novel selective Axl inhibitors. One of the most promising compounds **8i** tightly bound with Axl and suppressed Axl kinase activity with a K_d value of 1.1 nM and an IC_{50} value of 26 nM, respectively,

but it is significantly less potent for a panel of 403 nonmutated kinases evaluated at 1.0 μM (which is approximately 909 times higher than its K_d value against Axl) with the exception of Flt3. Thus, to the best of our knowledge, **8i** represents one of the most selective Axl inhibitors to date. **8i** also demonstrated reasonable PK properties and potently inhibit the phosphorylation levels of Axl. Furthermore, **8i** dose dependently blocked TGF- β 1 induced EMT and suppressed tumor invasion and migration in MDA-MB-231 breast cancer cells. Its strong Axl binding affinity and excellent target selectivity make compound **8i** not only a promising lead compound for drug discovery but also a valuable research probe for further biological investigation of its target.

5. Experimental Section

5.1 General methods for chemistry

All reagents and solvents were purchased from commercial sources without further purification. Flash chromatography was performed using 300 mesh silica gel. All reactions were monitored by TLC using silica gel plates with fluorescence F254 and UV light visualization. ^1H NMR spectra was recorded on a Bruker AV-400 spectrometer at 400 MHz or a Bruker AV-500 spectrometer at 500 MHz. ^{13}C NMR spectra was recorded on a Bruker AV-500 spectrometer at 125 MHz. Coupling constants (J) are expressed in hertz (Hz). Chemical shifts (δ) of NMR are reported in parts per million (ppm) units relative to an internal standard (TMS). Low resolution ESI-MS were recorded on an Agilent 1200 HPLC-MSD mass spectrometer and high resolution ESI-MS on an Applied Biosystems Q-STAR Elite ESI-LC-MS/MS mass spectrometer. Purity of compounds was determined by reverse-phase high performance liquid chromatography [HPLC, Dionex Summit HPLC (Column: Diamonsil C18, 5.0 μm , 4.6 \times 250 mm (Dikma Technologies); detector: PDA-100 photodiode array; injector: ASI-100 autoinjector; pump: p-680A)] to be >95%. A flow rate of 1.0 mL/min was used with mobile phase of MeOH in H_2O with 0.1% modifier (ammonia, v/v).

***N*-(4-((6,7-dimethoxyquinazolin-4-yl)oxy)-3-fluorophenyl)-6-ethyl-1,2-dimethyl-7-(4-methylpiperazin-1-yl)-4-oxo-1,4-dihydroquinoline-3-carboxamide (6)**

Compound **6** was prepared by following a procedure similar to that of **8i**. ^1H NMR (500 MHz, $\text{DMSO}-d_6$) δ 11.19 (s, 1H), 8.57 (s, 1H), 8.08 (s, 1H), 7.95 (dd, $J = 13.3, 2.2$ Hz, 1H), 7.59 (s, 1H), 7.49 (d, $J = 8.9$ Hz, 1H), 7.44 (d, $J = 8.6$ Hz, 1H), 7.42 (s, 1H), 4.00 (s, 3H), 3.99 (s, 3H), 3.82 (s, 3H), 3.03 (m, 4H), 2.74 (q, $J = 7.5$ Hz, 2H), 2.66 (s, 3H), 2.54 (m, 4H), 2.27 (s, 3H), 1.27 (t, $J =$

7.5 Hz, 3H). ^{13}C NMR (125 MHz, $\text{DMSO-}d_6$) δ 173.67, 166.23, 164.58, 156.42, 156.11, 152.71, 152.60, 150.77, 149.45, 140.62, 138.92 (d, $J = 10.9$ Hz, 1C), 135.14, 134.80 (d, $J = 13.0$ Hz, 1C), 125.80, 124.80, 121.67, 118.29, 115.98, 109.62, 108.06, 107.28, 106.50, 101.06, 56.68, 56.56, 55.47, 52.10, 46.28, 35.62, 23.09, 19.57, 14.94. HRMS (ESI) for $\text{C}_{32}\text{H}_{28}\text{F}_2\text{N}_6\text{O}_5\text{S}$ $[\text{M}+\text{H}]^+$, calcd: 641.2854, found: 641.2882. HPLC analysis: MeOH- H_2O (85:15), 10.76 min, 97.64% purity.

Cyclopropyl-*N*-(4-((6,7-dimethoxyquinazolin-4-yl)oxy)-3-fluorophenyl)-6-fluoro-4-oxo-7-(piperazin-1-yl)-1,4-dihydroquinoline-3-carboxamide (8a)

A mixture of 4-((6,7-dimethoxyquinazolin-4-yl)oxy)-3-fluoroaniline (**11**, 100mg, 1 mmol), 7-(4-(tert-butoxycarbonyl)piperazin-1-yl)-1-cyclopropyl-6-fluoro-4-oxo-1,4-dihydroquinoline-3-carboxylic acid (**7a**) (150 mg, 1.1 mmol), HATU (180 mg, 1.5 mmol), and DIPEA (0.16 mL, 3 mmol) in DMF (20 mL) was stirred at rt overnight. Next, water was added to the mixture, and the precipitates were filtrated. The filter cake was washed with water, diluted with DCM, and concentrated in vacuo. The resulting residue was purified by flash chromatography on silica gel to get the product as a white solid. The resulting compound (150 mg) was dissolved in 10 mL DCM, 5 mL F_3CCOOH was added slowly under ice bath, then stirred at rt overnight. The organic solvent was removed under vacuum, and the resulting residue was washed by saturated NaOH, then water was added to the residue. The precipitate was filtered and washed with EA and acetone to give the white product (100 mg, 78%). ^1H NMR (500 MHz, CDCl_3) δ 12.50 (s, 1H), 8.89 (s, 1H), 8.62 (s, 1H), 8.05 (d, $J = 13.5$ Hz, 1H), 8.00 (dd, $J_1 = 2.0$ Hz, $J_2 = 12.0$ Hz, 1H), 7.58 (s, 1H), 7.46 (d, $J = 9.0$ Hz, 1H), 7.34 (m, 2H), 7.26 (s, 1H), 4.07 (s, 3H), 4.06 (s, 3H), 3.52 (m, 1H), 3.28 (t, $J = 4.5$ Hz, 4H), 3.10 (t, $J = 4.5$ Hz, 4H), 1.37 (m, 2H), 1.22 (m, 2H). ^{13}C NMR (125 MHz, CDCl_3) δ 175.57, 164.87, 163.18, 155.96, 154.26 (d, $J = 246.3$ Hz, 1C), 153.66 (d, $J = 248.5$ Hz, 1C), 152.89, 150.29, 149.44, 147.04, 145.69 (d, $J = 10.1$ Hz, 1C), 138.61, 137.80 (d, $J = 9.8$ Hz, 1C), 135.32 (d, $J = 12.6$ Hz, 1C), 123.82, 121.43 (d, $J = 7.3$ Hz, 1C), 116.09 (d, $J = 3.0$ Hz, 1C), 112.68 (d, $J = 23.3$ Hz, 1C), 110.98, 110.31, 109.28 (d, $J = 23.0$ Hz, 1C), 106.83, 104.67 (d, $J = 2.8$ Hz, 1C), 101.10, 56.41, 56.39, 51.17, 51.14, 45.97, 35.01, 8.24. HRMS (ESI) for $\text{C}_{33}\text{H}_{30}\text{F}_2\text{N}_6\text{O}_5$ $[\text{M}+\text{H}]^+$, calcd: 629.2319, found: 629.2306. HPLC analysis: MeOH- H_2O (85:15), 17.78 min, 97.22% purity.

1-cyclopropyl-N-(4-((6,7-dimethoxyquinazolin-4-yl)oxy)-3-fluorophenyl)-7-(4-ethylpiperazin-1-yl)-6-fluoro-4-oxo-1,4-dihydroquinoline-3-carboxamide (8b)

The compound was prepared by following a procedure similar to that of **8i**. ^1H NMR (500 MHz, CDCl_3) δ 12.50 (s, 1H), 8.89 (s, 1H), 8.63 (s, 1H), 8.06 (d, $J = 13.5$ Hz, 1H), 8.00 (dd, $J_1 = 2.5$ Hz, $J_2 = 12.5$ Hz, 1H), 7.58 (s, 1H), 7.46 (dd, $J_1 = 0.5$ Hz, $J_2 = 8.5$ Hz, 1H), 7.36 (m, 1H), 7.33 (s, 1H), 7.28 (m, 1H), 4.08 (s, 3H), 4.06 (s, 3H), 3.52 (m, 1H), 3.35 (t, $J = 4.5$ Hz, 4H), 2.69 (s, 4H), 2.52 (q, $J = 7.0$ Hz, 2H), 1.36 (m, 2H), 1.21 (m, 2H), 1.15 (t, $J = 7.0$ Hz, 3H). ^{13}C NMR (125 MHz, CDCl_3) δ 175.55, 164.86, 163.15, 155.94, 154.26 (d, $J = 246.1$ Hz, 1C), 153.64 (d, $J = 248.6$ Hz, 1C), 152.92, 150.28, 149.46, 147.03, 145.33 (d, $J = 10.4$ Hz, 1C), 138.59, 137.82 (d, $J = 9.9$ Hz, 1C), 135.32 (d, $J = 13.0$ Hz, 1C), 123.80, 121.47 (d, $J = 7.3$ Hz, 1C), 116.07 (d, $J = 2.6$ Hz, 1C), 112.66 (d, $J = 23.1$ Hz, 1C), 111.01, 110.32, 109.26 (d, $J = 23.3$ Hz, 1C), 106.86, 104.72, 104.70, 101.10, 56.40, 56.38, 52.53, 52.31, 50.00, 49.96, 34.99, 11.99, 8.23. HRMS (ESI) for $\text{C}_{35}\text{H}_{34}\text{F}_2\text{N}_6\text{O}_5$ $[\text{M}+\text{H}]^+$, calcd: 657.2632, found: 657.2625. HPLC analysis: MeOH- H_2O (85:15), 20.53 min, 98.36% purity.

N-(4-((6,7-dimethoxyquinazolin-4-yl)oxy)-3-fluorophenyl)-1-ethyl-6,8-difluoro-7-(3-methylpiperazin-1-yl)-4-oxo-1,4-dihydroquinoline-3-carboxamide (8c)

A mixture of 4-((6,7-dimethoxyquinazolin-4-yl)oxy)-3-fluoroaniline (**11**, 315 mg, 1.0 mmol), 7-(4-(tert-butoxycarbonyl)-3-methylpiperazin-1-yl)-1-ethyl-6,8-difluoro-4-oxo-1,4-dihydroquinoline-3-carboxylic acid (**7c**, 490 mg, 1.0 mmol), HATU (574 mg, 1.5 mmol), and DIPEA (0.5 mL, 3 mmol) in DMF (20 mL) was stirred at rt overnight. Next, water was added to the mixture, and the precipitates were filtrated. The filter cake was washed with water, diluted with DCM, and concentrated in vacuo. The product was then dissolved in 10 mL DCM, 5 mL F_3CCOOH was added slowly under ice bath and stirred at rt overnight. The organic solvent was removed under vacuum, and the resulting residue was alkalinized by saturated NaOH. The precipitate was filtered and washed with EA and acetone to give the white product (485 mg, 75%). ^1H NMR (400 MHz, d_6 -DMSO) ^1H NMR (400 MHz, $\text{DMSO}-d_6$) δ 12.36 (s, 1H), 8.93 (s, 1H), 8.56 (s, 1H), 7.99 (dd, $J = 12.0$, 1.6 Hz, 1H), 7.94 (dd, $J = 12.0$, 1.6 Hz, 1H), 7.56 (s, 1H), 7.51-7.45 (m, 2H), 7.40 (s, 1H), 4.62-4.57 (m, 2H), 4.00 (s, 3H), 3.98 (s, 3H), 3.58 (m, 2H), 3.49-3.40 (m, 3H), 3.29-3.17 (m, 2H), 1.48-1.45 (m, 3H), 1.26 (d, $J = 6.4$ Hz, 3H). ^{13}C NMR (125 MHz, d_6 -DMSO) δ 173.87, 164.49, 162.76, 158.70, 158.45, 156.43, 154.09 (d, $J = 243.4$ Hz, 1C),

153.85, 152.57, 151.17, 150.76, 149.44, 137.83 (d, $J = 10.3$ Hz, 1C), 135.26 (d, $J = 13.1$ Hz, 1 C), 132.29 (d, $J = 13.6$ Hz, 1C), 127.141 (d, $J = 6.9$ Hz, 1C), 125.11, 123.73 (d, $J = 8.0$ Hz, 1C), 116.50 (d, $J = 11.9$ Hz, 1C), 110.23, 109.59, 108.53 (d, $J = 22.9$ Hz, 1C), 107.56 (d, $J = 22.9$ Hz, 1C), 101.02, 56.69, 56.53, 53.93, 53.77, 51.46, 47.40, 43.59, 16.45 (d, $J = 4.9$ Hz, 1C), 15.83. HRMS (ESI) for $C_{33}H_{31}F_3N_6O_5$ $[M+H]^+$, calcd: 649.2333, found: 649.2361. HPLC analysis: MeCN-H₂O (70:30), 6.81 min, 97.43% purity.

***N*-(4-((6,7-dimethoxyquinazolin-4-yl)oxy)-3-fluorophenyl)-1-ethyl-6-fluoro-4-oxo-7-(piperazin-1-yl)-1,4-dihydro-1,8-naphthyridine-3-carboxamide (8d)**

The compound was prepared by following a procedure similar to that of **8a**. ¹H NMR (500 MHz, CDCl₃) δ 12.51 (s, 1H), 8.79 (s, 1H), 8.63 (s, 1H), 8.13 (d, $J = 13.5$ Hz, 1H), 7.80 (dd, $J_1 = 2.0$ Hz, $J_2 = 12.0$ Hz, 1H), 7.58 (s, 1H), 7.46 (d, $J = 8.5$ Hz, 1 H), 7.33 (s, 1H), 7.28 (m, 1H), 4.41 (q, $J = 7.0$ Hz, 2H), 4.08 (s, 3H), 4.06 (s, 3H), 3.82 (t, $J = 4.5$ Hz, 4H), 3.04 (t, $J = 4.5$ Hz, 4H), 1.82 (s, 1H), 1.51 (t, $J = 7.0$ Hz, 3H). ¹³C NMR (125 MHz, CDCl₃) δ 175.65, 164.86, 163.05, 155.95, 154.26 (d, $J = 245.9$ Hz, 1C), 152.91, 150.37 (d, $J = 9.0$ Hz, 1C), 150.28, 149.46, 147.36 (d, $J = 257.0$ Hz, 1C), 146.02, 144.65, 137.80 (d, $J = 9.6$ Hz, 1C), 135.34 (d, $J = 13.1$ Hz, 1C), 123.81, 120.66 (d, $J = 21.9$ Hz, 1C), 116.10 (d, $J = 2.9$ Hz, 1C), 115.11 (d, $J = 3.0$ Hz, 1C), 112.20, 110.32, 109.29 (d, $J = 23.3$ Hz, 1C), 106.86, 101.10, 56.40, 56.38, 48.38, 48.32, 47.44, 46.11, 15.03. HRMS (ESI) for $C_{31}H_{29}F_2N_7O_5$ $[M+H]^+$, calcd: 618.2271, found: 618.2264. HPLC analysis: MeOH-H₂O (85:15), 16.99 min, 96.81% purity.

5-amino-1-cyclopropyl-*N*-(4-((6,7-dimethoxyquinazolin-4-yl)oxy)-3-fluorophenyl)-7-((3*S*,5*R*)-3,5-dimethylpiperazin-1-yl)-6,8-difluoro-4-oxo-1,4-dihydroquinoline-3-carboxamide (8e)

The compound was prepared by following a procedure similar to that of **8i**. ¹H NMR (500 MHz, *d*₆-DMSO) δ 12.19 (s, 1H), 8.58 (s, 1H), 8.53 (s, 1H), 7.96 (d, $J = 12.5$ Hz, 1H), 7.55 (s, 1H), 7.44-7.37 (m, 5H), 3.98 (s, 3H), 3.97 (s, 3H), 3.34 (d, $J = 12.0$ Hz, 2H), 3.10 (s, 2H), 2.92 (t, $J = 11.5$ Hz, 2H), 1.90 (s, 2H), 1.13-1.07 (m, 10H). ¹³C NMR (125 MHz, *d*₆-DMSO) δ 178.94, 172.67, 164.49, 162.77, 156.42, 154.03 (d, $J = 243.3$ Hz, 1C), 152.56, 150.73, 149.67, 149.38, 139.76 (d, $J = 230.5$ Hz, 1C), 137.85 (d, $J = 9.75$ Hz, 1C), 136.92 (d, $J = 13.3$ Hz, 1C), 135.11 (d, $J = 13.1$ Hz, 1C), 133.20, 128.35, 124.96, 116.46, 109.58, 109.15, 108.50 (d, $J = 23.5$ Hz, 1C), 107.28, 107.15, 101.00, 56.66, 56.50, 56.05, 21.59, 17.94, 9.01, 8.95. HRMS (ESI) for

$C_{35}H_{34}F_3N_7O_5$ $[M+H]^+$, calcd: 690.2646, found: 690.2622. HPLC analysis: MeOH-H₂O (90:10), 10.22 min, 95.56% purity.

***N*-(4-((6,7-dimethoxyquinazolin-4-yl)oxy)-3-fluorophenyl)-6,8-difluoro-1-(2-fluoroethyl)-7-(4-methylpiperazin-1-yl)-4-oxo-1,4-dihydroquinoline-3-carboxamide (8f)**

The compound was prepared by following a procedure similar to that of **8i**. ¹H NMR (500 MHz, *d*₆-DMSO) δ 12.35 (s, 1H), 8.84 (s, 1H), 8.57 (s, 1H), 8.00 (d, *J* = 12.5 Hz, 1H), 7.88 (d, *J* = 12.0 Hz, 1H), 7.57 (s, 1H), 7.48 (m, 2H), 7.41 (s, 1H), 4.95-4.86 (m, 4H), 4.00 (s, 3H), 3.99 (s, 3H), 3.33 (s, 4H), 2.45 (s, 4H), 2.23 (s, 3H). ¹³C NMR (125 MHz, CDCl₃) δ 174.61, 164.83, 162.44, 155.97, 155.01 (d, *J* = 249.0 Hz, 1C), 154.27 (d, *J* = 246.3 Hz, 1C), 152.88, 150.87, 150.30, 149.47, 145.94 (dd, *J*₁ = 6.4 Hz, *J*₂ = 244.4 Hz, 1C), 137.54 (d, *J* = 9.5 Hz, 1C), 135.51 (d, *J* = 13.0 Hz, 1C), 133.82 (t, *J* = 13.8 Hz, 1C), 126.58 (d, *J* = 5.2 Hz, 1C), 123.87, 122.87 (d, *J* = 7.9 Hz, 1C), 116.12 (d, *J* = 2.8 Hz, 1C), 111.03, 110.30, 109.33 (d, *J* = 23.1 Hz, 1C), 108.81 (d, *J* = 22.9 Hz, 1C), 106.86, 101.08, 81.25 (dd, *J*₁ = 5.4 Hz, *J*₂ = 172.3 Hz, 1C), 58.30 (dd, *J*₁ = 14.9 Hz, *J*₂ = 20.4 Hz, 1C), 56.40, 56.38, 55.52, 50.89 (t, *J* = 4.0 Hz, 2C), 46.34. HRMS (ESI) for $C_{33}H_{30}F_4N_6O_5$ $[M+H]^+$, calcd: 667.2287, found: 667.2290. HPLC analysis: MeOH-H₂O (85:15), 14.66 min, 99.56% purity.

***N*-(4-((6,7-dimethoxyquinazolin-4-yl)oxy)-3-fluorophenyl)-6-fluoro-1-(4-fluorophenyl)-4-oxo-7-(piperazin-1-yl)-1,4-dihydroquinoline-3-carboxamide (8g)**

The compound was prepared by following a procedure similar to that of **8a**. ¹H NMR (500 MHz, *d*₆-DMSO) δ 12.51 (s, 1H), 8.61 (s, 1H), 8.54 (s, 1H), 7.96 (m, 1H), 7.92 (d, *J* = 13.0 Hz, 1H), 7.81 (m, 2H), 7.55 (m, 3H), 7.45 (m, 2H), 7.39 (s, 1H), 3.98 (s, 3H), 3.97 (s, 3H), 2.91 (s, 4H), 2.77 (s, 4H). ¹³C NMR (125 MHz, *d*₆-DMSO) δ 179.96, 169.27, 167.73, 167.65 (d, *J* = 246.1 Hz, 1C), 161.20, 158.84 (d, *J* = 243.5 Hz, 1C), 158.03 (d, *J* = 247.0 Hz, 1C), 157.33 (d, *J* = 24.4 Hz, 1C), 155.53, 154.21, 152.94 (d, *J* = 23.1 Hz, 1C), 150.41 (d, *J* = 10.4 Hz, 1C), 143.81, 142.61 (d, *J* = 9.8 Hz, 1C), 141.87, 140.00 (d, *J* = 12.9 Hz, 1C), 135.11, 129.81, 125.13 (d, *J* = 7.3 Hz, 1C), 122.58 (d, *J* = 23.4 Hz, 1C), 121.18, 116.58, 115.24, 114.37, 113.28, 112.03, 111.17, 105.79 (d, *J* = 12.6 Hz, 1C), 61.43, 61.27, 55.73, 50.46. HRMS (ESI) for $C_{36}H_{29}F_3N_6O_5$ $[M+H]^+$, calcd: 683.2224, found: 683.2226. HPLC analysis: MeOH-H₂O (85:15), 13.93 min, 95.12% purity.

7-(3-aminopyrrolidin-1-yl)-1-(2,4-difluorophenyl)-N-(4-((6,7-dimethoxyquinazolin-4-yl)oxy)-3-fluorophenyl)-6-fluoro-4-oxo-1,4-dihydro-1,8-naphthyridine-3-carboxamide (8h)

The compound was prepared by following a procedure similar to that of **8a**. ¹H NMR (500 MHz, *d*₆-DMSO) δ 12.52 (s, 1H), 8.75 (s, 1H), 8.57 (s, 1H), 8.06 (d, *J* = 13.0 Hz, 1H), 7.98 (d, *J* = 12.5 Hz, 1H), 7.85 (m, 1H), 7.59 (m, 2H), 7.47 (d, *J* = 12.5 Hz, 2 H), 7.41 (s, 1H), 7.36 (t, *J* = 8.0 Hz, 1H), 4.62 (s, 2H), 4.00 (s, 3H), 3.99 (s, 3H), 3.62 (m, 5H), 2.02 (s, 1H), 1.76 (s, 1H). ¹³C NMR (125 MHz, CDCl₃) δ 176.04 (d, *J* = 1.6 Hz, 1C), 164.78, 163.03 (dd, *J*₁ = 10.9 Hz, *J*₂ = 251.1 Hz, 1C), 162.59, 157.83 (dd, *J*₁ = 12.4 Hz, *J*₂ = 253.9 Hz, 1C), 155.96, 154.19 (d, *J* = 246.1 Hz, 1C), 152.77, 150.29, 149.38, 148.92 (d, *J* = 12.6 Hz, 1C), 146.39 (d, *J* = 256.3 Hz, 1C), 146.15, 145.98, 137.62 (d, *J* = 9.6 Hz, 1C), 135.36 (d, *J* = 13.3 Hz, 1C), 130.00 (d, *J* = 10.1 Hz, 1C), 124.72 (dd, *J*₁ = 4.3 Hz, *J*₂ = 13.3 Hz, 1C), 123.82, 118.45 (d, *J* = 20.6 Hz, 1C), 116.07 (d, *J* = 2.6 Hz, 1C), 112.69, 112.41 (d, *J* = 2.5 Hz, 1C), 112.01 (dd, *J*₁ = 3.4 Hz, *J*₂ = 22.5 Hz, 1C), 110.24, 109.20 (d, *J* = 23.0 Hz, 1C), 106.76, 104.94 (t, *J* = 23.5 Hz, 1C), 101.03, 56.61, 56.57, 56.38, 56.35, 46.92, 30.32. HRMS (ESI) for C₃₅H₂₇F₄N₇O₅ [M+H]⁺, calcd: 702.2083, found: 702.2074. HPLC analysis: MeOH-H₂O (85:15), 12.42 min, 99.81% purity.

N-(4-((6,7-dimethoxyquinazolin-4-yl)oxy)-3-fluorophenyl)-9-fluoro-8-(4-hydroxypiperidin-1-yl)-5-methyl-1-oxo-1,5,6,7-tetrahydropyrido[3,2,1-*ij*]quinoline-2-carboxamide. (8i)

A mixture of 4-((6,7-dimethoxyquinazolin-4-yl)oxy)-3-fluoroaniline (**11**, 315 mg, 1 mmol), Nadifloxacin (433 mg, 1.2 mmol), HATU (570 mg, 1.5 mmol), and DIEA (0.5 mL, 3 mmol) in DMF (20 mL) was stirred at rt overnight. Next, water was added to the mixture, and the precipitates was filtrated. The filter cake was washed with water, diluted with DCM, and concentrated in vacuo. The resulting residue was purified by flash chromatography on silica gel to get the product as a white solid (460 mg, 70 %). ¹H NMR (500 MHz, *d*₆-DMSO) δ 12.66 (s, 1H), 8.95 (s, 1H), 8.57 (s, 1H), 8.02 (d, *J* = 13.0 Hz, 1H), 7.89 (d, *J* = 13.0 Hz, 1H), 7.58 (s, 1H), 7.48 (m, 2H), 7.41 (s, 1H), 4.87 (s, 1H), 4.75 (s, 1H), 4.00 (s, 3H), 3.99 (s, 3H), 3.68 (s, 1H), 3.20-3.13 (m, 3H), 2.96-2.92 (m, 2H), 2.16-2.06 (m, 2H), 1.90-1.83 (m, 2H), 1.63-1.50 (m, 2H), 1.43 (d, *J* = 6.5 Hz, 3H). ¹³C NMR (125 MHz, *d*₆-DMSO) δ 175.04, 164.47, 163.30, 157.47 (d, *J* = 247.3 Hz, 1C), 156.41, 154.04 (d, *J* = 243.5 Hz, 1C), 152.51, 150.74, 149.41, 147.12, 142.33 (d, *J* = 13.6 Hz, 1C), 138.01

(d, $J = 9.4$ Hz, 1C), 135.06 (d, $J = 12.9$ Hz, 1C), 133.57, 126.65, 124.92, 124.13 (d, $J = 8.1$ Hz, 1C), 116.22, 109.79, 109.60, 109.56, 108.37 (d, $J = 23.1$ Hz, 1C), 107.21, 101.03, 57.09, 56.60, 56.46, 49.08, 35.86, 35.50, 25.58, 20.05, 18.94. HRMS (ESI) for $C_{35}H_{33}F_2N_5O_6$ $[M+H]^+$, calcd: 658.2424, found: 658.2416. HPLC analysis: MeOH-H₂O (85:15), 10.63 min, 99.51% purity. MW: 657.66, cLogP: 3.314, tPSA: 125.29.

***N*-(4-(((6,7-dimethoxyquinazolin-4-yl)oxy)-3-fluorophenyl)-9-fluoro-3-methyl-10-(4-methylpiperazin-1-yl)-7-oxo-3,7-dihydro-2*H*-[1,3,4]oxadiazino[6,5,4-*ij*] quinolone-6-carboxamide (8j).**

The compound was prepared by following a procedure similar to that of **8i**. ¹H NMR (500 MHz, *d*₆-DMSO) δ 12.47 (s, 1H), 8.73 (s, 1H), 8.56 (s, 1H), 7.99 (m, 1H), 7.57 (m, 2H), 7.45 (m, 2H), 7.41 (s, 1H), 5.32 (s, 2H), 4.00 (s, 3H), 3.99 (s, 3H), 3.33 (m, 4H), 3.03 (s, 3H), 2.45 (s, 4H), 2.24 (s, 3H). ¹³C NMR (125 MHz, *d*₆-DMSO) δ 174.54, 164.51, 162.78, 156.44, 155.69 (d, $J = 244.5$ Hz, 1C), 154.08 (d, $J = 243.5$ Hz, 1C), 152.59, 150.77, 149.46, 144.71, 138.66 (d, $J = 7.4$ Hz, 1C), 137.88 (d, $J = 10.0$ Hz, 1C), 135.20 (d, $J = 12.8$ Hz, 1C), 131.45 (d, $J = 14.1$ Hz, 1C), 125.07, 123.89, 121.49 (d, $J = 8.1$ Hz, 1C), 116.39, 109.60, 109.53, 108.48 (d, $J = 22.8$ Hz, 1C), 107.27, 104.45 (d, $J = 23.4$ Hz, 1C), 101.02, 82.64, 56.68, 56.52, 55.72, 50.54, 46.47, 43.22. HRMS (ESI) for $C_{33}H_{31}F_2N_7O_6$ $[M+H]^+$, calcd: 660.2377, found: 660.2373. HPLC analysis: MeOH-H₂O (85:15), 15.48 min, 99.89% purity.

***(S)*-(4-(((6,7-dimethoxyquinazolin-4-yl)oxy)-3-fluorophenyl)-9-fluoro-3-methyl-10-(4-methylpiperazin-1-yl)-7-oxo-3,7-dihydro-2*H*-[1,4]oxazino[2,3,4-*ij*]quinoline-6-carboxamide (8k)**

The compound was prepared by following a procedure similar to that of **8i**. ¹H NMR (500 MHz, *d*₆-DMSO) δ 12.59 (s, 1H), 8.95 (s, 1H), 8.57 (s, 1H), 8.00 (m, 1H), 7.58 (m, 2H), 7.46 (m, 2H), 7.40 (s, 1H), 4.92 (m, 1H), 4.57 (d, $J = 10.5$ Hz, 1H), 4.38 (d, $J = 9.5$ Hz, 1H), 4.00 (s, 3H), 3.99 (s, 3H), 3.33 (m, 4H), 2.63 (s, 4H), 2.37 (s, 3H), 1.47 (d, $J = 7.0$ Hz, 3H). ¹³C NMR (125 MHz, *d*₆-DMSO) δ 174.84, 164.52, 163.30, 156.43, 155.78 (d, $J = 244.0$ Hz, 1C), 154.09 (d, $J = 243.5$ Hz, 1C), 152.59, 150.76, 149.45, 146.00, 140.79 (d, $J = 7.1$ Hz, 1C), 138.02 (d, $J = 10.1$ Hz, 1C), 135.11 (d, $J = 12.9$ Hz, 1C), 131.39 (d, $J = 14.8$ Hz, 1C), 125.06, 124.81, 122.07 (d, $J = 8.6$ Hz, 1C), 116.36, 109.84, 109.60, 108.46 (d, $J = 22.9$ Hz, 1C), 107.27, 103.97 (d, $J = 23.3$ Hz, 1C), 101.02, 68.64, 56.68, 56.52, 55.39, 54.85, 50.01, 45.80, 18.36. HRMS (ESI) for $C_{34}H_{32}F_2N_6O_6$ $[M+H]^+$, calcd: 659.2424, found: 659.2425. HPLC analysis: MeOH-H₂O (85:15), 15.81

min, 98.54% purity.

***N*-(4-((6,7-dimethoxyquinazolin-4-yl)oxy)-3-fluorophenyl)-6-fluoro-1-methyl-4-oxo-7-(piperazin-1-yl)-1,4-dihydro-[1,3]thiazeto[3,2-*a*]quinoline-3-carboxamide (8I)**

The compound was prepared by following a procedure similar to that of **8a**. ¹H NMR (400 MHz, DMSO-*d*₆) δ 12.12 (s, 1H), 8.57 (s, 1H), 7.98-7.91 (m, 1H), 7.82 (d, *J* = 13.9 Hz, 1H), 7.58 (s, 1H), 7.44 (dd, *J* = 3.9, 1.6 Hz, 2H), 7.42 (s, 1H), 6.86 (d, *J* = 7.3 Hz, 1H), 6.36 (q, *J* = 6.1 Hz, 1H), 4.00 (s, 3H), 3.99 (s, 3H), 3.17 (t, *J* = 4.6 Hz, 4H), 2.94-2.82 (m, 4H), 2.11 (d, *J* = 6.1 Hz, 3H). ¹³C NMR (125 MHz, CDCl₃) δ 174.25, 164.81, 163.82, 162.12, 154.24 (d, *J* = 245.9 Hz, 1C), 153.62, 152.87, 151.65, 150.267, 149.44, 145.60 (d, *J* = 10.6 Hz, 1C), 137.38 (d, *J* = 10.0 Hz, 1C), 135.56, 135.35 (d, *J* = 13.3 Hz, 1C), 123.79 (d, *J* = 1.8 Hz, 1C), 120.75 (d, *J* = 7.4 Hz, 1C), 115.82 (d, *J* = 3.1 Hz, 1C), 114.05 (d, *J* = 23.5 Hz, 1C), 110.05 (d, *J* = 23.5 Hz, 1C), 106.84, 105.23, 101.07, 99.89, 69.37, 56.37, 56.36, 51.03, 51.00, 45.87, 21.28, 1.00. HRMS (ESI) for C₃₂H₂₈F₂N₆O₅S [M+H]⁺, calcd: 647.1883, found: 647.1882. HPLC analysis: MeOH-H₂O (80:20), 15.66 min, 96.78% purity.

5.2 Cell Culture and Reagents

MDA-MB-231 cells were purchased from American type culture collection (ATCC). MDA-MB-231 were maintained in Roswell Park Memorial Institute (RPMI)-1640 supplemented with 10% fetal bovine serum (FBS), 100 U/mL penicillin, 50 mg/mL streptomycin, and 2 mmol/L glutamine in a humidified CO₂ incubator at 37 °C. All cells were passaged for less than 3 months before renewal from frozen, early-passage stocks obtained from the indicated sources.

The compound was dissolved in dimethyl sulfoxide (DMSO, Sigma-Aldrich) at a concentration of 10 mmol/L and stored at -20 °C. Primary antibodies against Ax1 (8661), phosphor-Ax1 (Tyr⁷⁰², 5724), E-cadherin (3195), N-cadherin (13116), glyceraldehyde-3-phosphate dehydrogenase (GAPDH, 2118) and anti-rabbit or anti-mouse IgG horseradish peroxidase (HRP)-linked secondary antibodies were purchased from Cell Signaling Technology (CST, Boston, MA, USA). Primary antibodies against v-akt murine thymoma viral oncogene homolog (AKT, SC8312), phosphor-AKT (SC16646R, SC7985R) were purchased from Santa Cruz Biotechnology (Santa Cruz, CA)

5.3 Animals

Male Sprague Dawley mice were obtained from the Animal Center of Jinan University. Animal

experiments were performed in accordance with the Guide for the Care and Use of Laboratory Animals. All animal experimental procedures were approved by the Jinan University Animal Policy and Welfare Committee.

5.4 *In Vitro* Enzymatic Activity Assay

Axl and the Z'-Lyte Kinase Assay Kit were purchased from Invitrogen. The experiments were performed according to the instructions of the manufacturer. The concentrations of kinases were determined by optimization experiments and the respective concentration was: Axl (PV3971, Invitrogen) 0.22 $\mu\text{g}/\mu\text{L}$. First, the compounds were diluted by three-fold from 10^{-10} M to 1×10^{-4} M in DMSO and a 400 μM of compound solution was prepared (4 μL compound dissolved in 96 μL water). Second, a 100 μM ATP solution in 1.33 \times Kinase Buffer was prepared. Third, a kinase/peptide mixture containing 2 \times kinase and 4 μM Tyr6 peptide (PV4122; Invitrogen) was prepared right before use. Kinase/peptide mixture was prepared by diluting Z'-LYTE Tyr6 peptide (PV4122; Invitrogen) and kinase in 1 \times Kinase Buffer, and 0.2 μM Tyr6 phospho-peptide solution was made by adding Z'-LYTE Tyr6 phospho-peptide to 1 \times Kinase Buffer. The final 10 μL reaction consists of 0.002 ng of Axl, 2 μM Tyr6 peptide in 1 \times kinase buffer. For each assay, 10 μL kinase reactions were made at first (including 2.5 μL compound solution, 5 μL Kinase/Peptide Mixture, and 2.5 μL ATP solution). Mixed the plate thoroughly and incubated for one hour at room temperature. Then 5 μL development solution was added to each well and the plate was incubated for 1.0 h at room temperature; the nonphosphopeptides were cleaved at this time. In the end, 5 μL stop reagent was loaded to stop the reaction. For the control setting, 5 μL phospho-peptide solution instead of kinase/peptide mixture was used as 100% phosphorylation control. 2.5 μL 1.33 \times Kinase Buffer instead of ATP solution was used as 100% inhibition control, and 2.5 μL 4% DMSO instead of compound solution was used as the 0% inhibitor control. The plate was measured on an EnVision Multilabel Reader (Perkin-Elmer). Curve fitting and data presentations were performed using Graph Pad Prism, version 5.0. Every experiment was repeated at least 2 times.

5.5 Western Blot Analysis

The western blot analysis was carried out by following the protocol described before. Briefly, after the indicated treatment, cell lysates were collected dissolving cells in 1 \times SDS sample lysis buffer (CST recommended). After being sonicated and boiled, the supernatant of cell lysate were

used for western blot analysis. Cell lysates were loaded to 8-12% SDS-PAGE and separated by electrophoresis. Separated proteins were then electrically transferred to a PVDF film. After being blocked with 1×TBS containing 0.5% Tween-20 and 5% non-fat milk, the film was incubated with corresponding primary antibody followed by HRP-conjugated secondary antibody. And the protein lanes were visualized using ECL Western Blotting Detection Kit (Thermo Scientific, USA).

5.6 Cell Migration and Invasion Assay

Cell migration assays were evaluated in Transwell chambers (Corning Costar). Cell invasion assays were evaluated in Magrigel invasion chambers (Corning Costar). $0.2\sim 1 \times 10^5$ tumor cells were plated in the top chamber with medium without FBS. RPMI-1640 medium containing 2% FBS with or without TGF- β 1 of 10 ng/ml and test compound (1.25~10 μ mol/L) was added to the bottom chamber. After incubation for 24 hrs at 37 °C, the cells were fixed in 100% methanol and stained with 0.25% crystal violet; and the cells that had not migrated from the top surface of the filters were removed with cotton. Migrated cells were quantitated by counting cells in six randomly selected fields on each filter under a microscope at 200 magnification and graphed as the mean of three independent experiments.

5.7 Determination of Pharmacokinetic Parameters in Rats

Compound **8i** was dissolved in 0.5% CMC-Na solvents. Male Sprague–Dawley rats (190–230 g) were dosed with the test compounds intravenously (iv) at 2.5 mg/kg and by oral gavage (po) at 25 mg/kg. Blood samples (0.2 mL) were then obtained via external jugular vein puncture at 0.25 h, 0.5 h, 1 h, 2 h, 4 h, 6 h, 8 h, 24 h time points and collected into heparinized tubes. Samples were centrifuged for cell removal, and the plasma supernatant was then transferred to a clean vial and subsequently stored in -80 °C prior to analysis. Test sample concentrations were determined by LC/MS and pharmacokinetic parameters were calculated using Analyst 1.5.1 software.

5.8 *In vivo* Acute Toxicity Study of compound **8i**

The ICR mice were randomly divided into an experimental group and a control group. Each group contains 6 mice (male). The experimental group mice were fed with **8i** solution once at a dose of 50, 100, 200, 400, 600 or 800 mg/kg. The control animals were treated with the same volume of vehicle. After administration, all animals were observed at 30 minutes, 1, 2, 4 and 6 hours, then during the remaining experimental period, for a total of 7 days. All animals were

observed at least once per day. The animals' body weight and survival were monitored every day. In addition, their histopathology was all measured at the final observation time points.

Acknowledgements

The authors thank the financial support from National Natural Science Foundation of China (21702074, 21572230, 81425021 and 81673285), Guangdong Natural Science Funds (2105A030312014), Guangdong Nanyue-Baijie Award, Guangzhou City Key Laboratory of Precision Chemical Drug Development (201805010007) and Jinan University (21616321).

Abbreviations

Mer, c-mer proto-oncogene tyrosine kinase; CML, chronic myeloid leukemia; Gas6, ligand growth arrest-specific 6; EMT, epithelial-mesenchymal transition; TNBC, triple negative breast cancer; EGFR, epidermal growth factor receptor; AML, acute myeloid leukemia; DHBA, dual hydrogen bond acceptor; NaH, Sodium hydride; DMF, *N,N*-dimethyl formamide; HATU, 1-[bis(dimethylamino)methylene]-1*H*-1,2,3-triazolo [4,5-*b*]pyridinium 3-oxid hexafluorophosphate; DIPEA, *N,N*-diisopropylethylamine; rt, room temperature; DCM, dichloromethane; Et3N, trimethylamine; DMAP, dimethylaminopyridine; (BOC)2O, Di-tert-butyl dicarbonate; FRET, fluorescence resonance energy transfer; IC₅₀, the half maximal (50%) inhibitory concentration of a substance; *K_d*, binding constant; CSF1R, colony stimulating factor 1 receptor; DDR, discoidin domain receptor; Flt3, FMS-like tyrosine kinase 3; Kit, v-kit Hardy-Zuckerman 4 feline sarcoma viral oncogene homolog; LOK, serine/threonine kinase 10; Trk, nerve growth factor receptor; TGF-β1, transforming growth factor β1; SD, Sprague-Dawley; PK, pharmacokinetic; AUC, Area Under The Curve.

References

- [1] Liu, E.; Hjelle, B.; Bishop, J. M., Transforming genes in chronic myelogenous leukemia. Proc. Natl. Acad. Sci. U S A. 85 (1988) 1952-1956.
- [2] Varnum, B. C.; Young, C.; Elliott, G.; Garcia, A.; Bartley, T. D.; Fridell, Y. W.; Hunt, R. W.; Trail, G.; Clogston, C.; Toso, R. J.; Yanagihara, D.; Bennett, L.; Sylber, M.; Merewether, L. A.; Tseng, A.; Escobar, E.; Liu, E. T.; Yamane, H. K., Axl receptor tyrosine kinase stimulated by the vitamin K-dependent protein encoded by growth-arrest-specific gene 6. Nature 373 (1995) 623-626.

- [3] Antony, J.; Huang, R. Y., AXL-Driven EMT State as a Targetable Conduit in Cancer. *Cancer Res.* 77 (2017) 3725-3732.
- [4] Li, Y.; Ye, X.; Tan, C.; Hongo, J. A.; Zha, J.; Liu, J.; Kallop, D.; Ludlam, M. J.; Pei, L., Axl as a potential therapeutic target in cancer: role of Axl in tumor growth, metastasis and angiogenesis. *Oncogene* 28 (2009) 3442-3455.
- [5] Postel-Vinay, S.; Ashworth, A., AXL and acquired resistance to EGFR inhibitors. *Nat. Genet.* 44 (2012) 835-836.
- [6] Shinh, Y.-S.; Lai, C.-Y.; Kao, Y.-R.; Shiah, S.-G.; Chu, Y.-W.; Lee, H.-S.; Wu, C.-W., Expression of Axl in Lung Adenocarcinoma and Correlation with Tumor Progression. *Neoplasia* 7 (2005) 1058-1064.
- [7] Ishikawa, M.; Sonobe, M.; Nakayama, E.; Kobayashi, M.; Kikuchi, R.; Kitamura, J.; Imamura, N.; Date, H., Higher expression of receptor tyrosine kinase Axl, and differential expression of its ligand, Gas6, predict poor survival in lung adenocarcinoma patients. *Ann. Surg. Oncol.* 20 (2013) S467-S476.
- [8] Bivona, T.; Okimoto, R., AXL receptor tyrosine kinase as a therapeutic target in NSCLC. *Lung Cancer (Auckl)* 6 (2015) 27-34.
- [9] Liu, L.; Greger, J.; Shi, H.; Liu, Y.; Greshock, J.; Annan, R.; Halsey, W.; Sathe, G. M.; Martin, A. M.; Gilmer, T. M., Novel mechanism of lapatinib resistance in HER2-positive breast tumor cells: activation of AXL. *Cancer Res.* 69 (2009) 6871-6878.
- [10] Skinner, H. D.; Giri, U.; Yang, L. P.; Kumar, M.; Liu, Y.; Story, M. D.; Pickering, C. R.; Byers, L. A.; Williams, M. D.; Wang, J.; Shen, L.; Yoo, S. Y.; Fan, Y. H.; Molkenline, D. P.; Beadle, B. M.; Meyn, R. E.; Myers, J. N.; Heymach, J. V., Integrative Analysis Identifies a Novel AXL-PI3 Kinase-PD-L1 Signaling Axis Associated with Radiation Resistance in Head and Neck Cancer. *Clin. Cancer Res.* 23 (2017) 2713-2722.
- [11] Myers, S. H.; Brunton, V. G.; and Unciti-Broceta, A., AXL Inhibitors in Cancer: A Medicinal Chemistry Perspective. *J. Med. Chem.* 59 (2016) 3593-3608.
- [12] Shin, J. S.; Hong, S. W.; Moon, J. H.; Kim, J. S.; Jung, K. A.; Kim, S. M.; Lee, D. H.; Kim, I.; Yoon, S. J.; Lee, C. G.; Choi, E. K.; Lee, J. Y.; Kim, K. P.; Hong, Y. S.; Lee, J. L.; Kim, B.; Choi, E. K.; Lee, J. S.; Jin, D. H.; Kim, T. W., NPS-1034, a novel MET inhibitor, inhibits the

activated MET receptor and its constitutively active mutants. *Invest. New Drugs* 32 (2014) 389-399.

[13] Ueno, Y.; Kaneko, N.; Saito, R.; Kondoh, Y.; Shimada, I.; Mori, M.; Kuromitsu, S., ASP2215, a novel FLT3/AXL inhibitor: Preclinical evaluation in combination with cytarabine and anthracycline in acute myeloid leukemia (AML). 2014 ASCO Annual Meeting.

[14] Mollard, A.; Warner, S. L.; Call, L. T.; Wade, M. L.; Bearss, J. J.; Verma, A.; Sharma, S.; Vankayalapati, H.; Bearss, D. J., Design, Synthesis and Biological Evaluation of a Series of Novel Axl Kinase Inhibitors. *ACS med. Chem. Lett.* 2 (2011) 907-912.

[15] Holland, S. J.; Pan, A.; Franci, C.; Hu, Y.; Chang, B.; Li, W.; Duan, M.; Torneros, A.; Yu, J.; Heckrodt, T. J.; Zhang, J.; Ding, P.; Apatira, A.; Chua, J.; Brandt, R.; Pine, P.; Goff, D.; Singh, R.; Payan, D. G.; Hitoshi, Y., R428, a selective small molecule inhibitor of Axl kinase, blocks tumor spread and prolongs survival in models of metastatic breast cancer. *Cancer Res.* 70 (2010) 1544-1554.

[16] <https://clinicaltrials.gov/ct2/show/NCT02488408>

[17] <https://clinicaltrials.gov/ct2/show/NCT02424617>

[18] Myers, S. H.; Temps, C.; Houston, D. R.; Brunton, V. G.; Unciti-Broceta, A., Development of Potent Inhibitors of Receptor Tyrosine Kinases by Ligand-Based Drug Design and Target-Biased Phenotypic Screening. *J Med. Chem.* 61 (2018) 2104-2110.

[19] Tan, L.; Zhang, Z.; Gao, D.; Luo, J.; Tu, Z. C.; Li, Z.; Peng, L.; Ren, X.; Ding, K., 4-Oxo-1,4-dihydroquinoline-3-carboxamide Derivatives as New Axl Kinase Inhibitors. *J. Med. Chem.* 59 (2016) 6807-6825.

[20] Singh, S.; Kaur, G.; Mangla, V.; Gupta, M. K., Quinoline and quinolones: promising scaffolds for future antimycobacterial agents. *J. Enzyme Inhib. Med. Chem.* 30 (2015) 492-504.

[21] Liu, K. K.; Sakya, S. M.; O'Donnell, C. J.; Li, J., Synthetic approaches to the 2008 new drugs. *Mini. Rev. Med. Chem.* 9 (2009) 1655-1675.

[22] Rodems, S. M.; Hamman, B. D.; Lin, C.; Zhao, J.; Shah, S.; Heidary, D.; Makings, L.; Stack, J. H.; Pollok, B. A. A FRET-based assay platform for ultra-high density drug screening of protein kinases and phosphatases. *Assay Drug Dev. Technol.* 1 (2002) 9-19.

[23] Karaman, M. W.; Herrgard, S.; Treiber, D. K.; Gallant, P.; Atteridge, C. E.; Campbell, B. T.; Chan, K. W.; Ciceri, P.; Davis, M. I.; Edeen, P. T.; Faraoni, R.; Floyd, M.; Hunt, J. P.; Lockhart, D.

J.; Milanov, Z. V.; Morrison, M. J.; Pallares, G.; Patel, H. K.; Pritchard, S.; Wodicka, L. M.; Zarrinkar, P. P., A quantitative analysis of kinase inhibitor selectivity. *Nat. Biotechnol.* 26 (2008) 127-32.

[24] Gjerdrum, C.; Tiron, C.; Hoiby, T.; Stefansson, I.; Haugen, H.; Sandal, T.; Collett, K.; Li, S.; McCormack, E.; Gjertsen, B. T.; Micklem, D. R.; Akslen, L. A.; Glackin, C.; Lorens, J. B., Axl is an essential epithelial-to-mesenchymal transition-induced regulator of breast cancer metastasis and patient survival. *Proc. Natl. Acad. Sci. U S A.* 107 (2010) 1124-1129.

[25] Wu, J.; Ru, N. Y.; Zhang, Y.; Li, Y.; Wei, D.; Ren, Z.; Huang, X. F.; Chen, Z. N.; Bian, H., HAb18G/CD147 promotes epithelial-mesenchymal transition through TGF-beta signaling and is transcriptionally regulated by Slug. *Oncogene* 30 (2011) 4410-4427.

1. Quinolone **8i** bound tightly to Axl with a K_d value of 1.1 nM
2. **8i** dose dependently inhibited cell invasion and migration in TGF- β 1 induced breast cancer cells.
3. **8i** exhibited extraordinary target selectivity over 468 kinases with a S(10) and S(35) value of 0.022 and 0.42 at 1.0 μ M, respectively.

ACCEPTED MANUSCRIPT